

DESIGN OF A CRANKSHAFT FOR INTERNAL COMBUSTION ENGINE BY USING TOPOLOGY OPTIMIZATION

Gustavo Rocha da Silva Santos, gustavo.dass@gmail.com

Guilherme Vinícius França dos Santos, guifranca@globocom

Emílio Carlos Nelli Silva, ecnsilva@usp.br

Escola Politécnica da Universidade de São Paulo, Av. Prof. Mello Moraes, 2231, 05508-900, São Paulo, SP, Brazil

Sergio Gradella Villalva, sergio.villalva@thyssenkrupp.com

Luis Antonio Fonseca Galli, luis.galli@thyssenkrupp.com

ThyssenKrupp Metalúrgica Campo Limpo – Av. Alfried Krupp, 1050 – Campo Limpo Paulista – SP - Brasil

Abstract. *This work presents the design of a crankshaft for a lightweight mono-cylinder spark-ignition four-stroke internal combustion engine using topology optimization. The topology optimization method implies the use of FE analysis combined with an optimization algorithm to find the optimum mass distribution of the crankshaft to minimize the component weight while satisfying manufacturing and maximum stress (yield strength) constraints. In addition, the application of this method allows control over the crankshaft natural frequencies by avoiding a spectrum around a specified eigenfrequency where no resonance occurs. This leads to a reduction of its torsional vibration, which is the leading cause of crankshaft failure. This methodology modifies the traditional mechanical design by placing structural analysis before the CAD design. The project includes the evaluation of the loads applied to the component through dynamical simulation of the cranktrain mechanism, including secondary motions of the connecting rod and the piston, while the gas force inputs are obtained from the combustion chamber simulation. Both dynamical and combustion simulations are performed using Ricardo Inc softwares. First, the topology optimization is applied to minimize the component weight and to tailor its natural frequencies. Following, a shape optimization is applied to reduce stress concentration. The optimization is implemented using the software Altair OptiStructTM, as the optimization and finite element solver and Altair HypermeshTM, as the mesh generator. The final crankshaft design is submitted to a durability analysis using the software EngdynTM from Ricardo Inc. This paper presents only the loads obtained analytically and the first optimization results.*

Keywords: *topology optimization; finite element analysis; internal combustion engine; crankshaft.*

1. INTRODUCTION

The increasing demand for fuel efficient internal combustion engines leads to research and application of innovative techniques in the structural design of its internal components. The topology optimization method allows the design with the optimum mass distribution by combining a finite element analysis with an optimization algorithm dedicated to minimize a given response, such as the compliance or the volume of the component (Bendsøe, Sigmund, 2003). Therefore the application of the method allows a more suitable design, allowing larger efficiency of the engine.

The crankshaft is one of the mechanical components of an internal combustion engine responsible for the conversion of the piston linear movement into rotational movement, thus making torque available for use at the shaft end. The component is subjected to complex loads, which combines time dependant forces, flexional (in-plane) and torsional (out-of-plane) moments, inertial forces and excitations due to vibration (Mendes, Meirelles, Zampiere, 2005). The loads are therefore highly dependent on the design of the component and at each iteration of the optimization some of the loads must be re-evaluated.

Montazersadgh and Fatemi (2007) performed size and shape optimization with manufacturing constraints on the crankweb and counterweight of a crankshaft, considering multiple load cases. Ganpule, Mate and Gokhale (2006) performed topology optimization with maximum stress constraint and shape optimization in a crankweb for a single static load, neglecting inertial effects.

1.1. The Engine

The engine that is modeled is a lightweight, four-stroke, spark ignition, monocyliner engine. Table 1 presents the engine and the crankshaft specification.

The original crankshaft is comprised by three parts with the crankpin being an independent component assembled through interference fit in the crankwebs. Figure 1 presents an off scale image of the digitized components of the crankshaft, except for the crankpin.

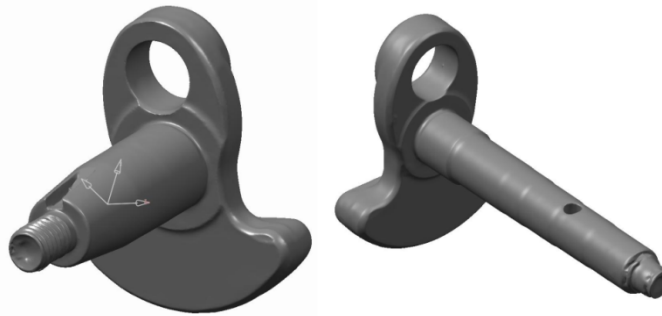


Figure1. Digitized components of the crankshaft.

Table 1. Engine data.

Number of Cylinders	1
Stroke	30mm
Displacement	35.8cm ³
Compression ratio	12:1
Net power output	1.2kW @ 7000rpm
Net torque	1.9Nm @ 5000rpm
Lubricating oil	SAE 20W50
Speed range	4,000rpm a 8,000rpm
Crankshaft mass ⁽¹⁾	176g

⁽¹⁾: Mass equivalent to the optimization domain.

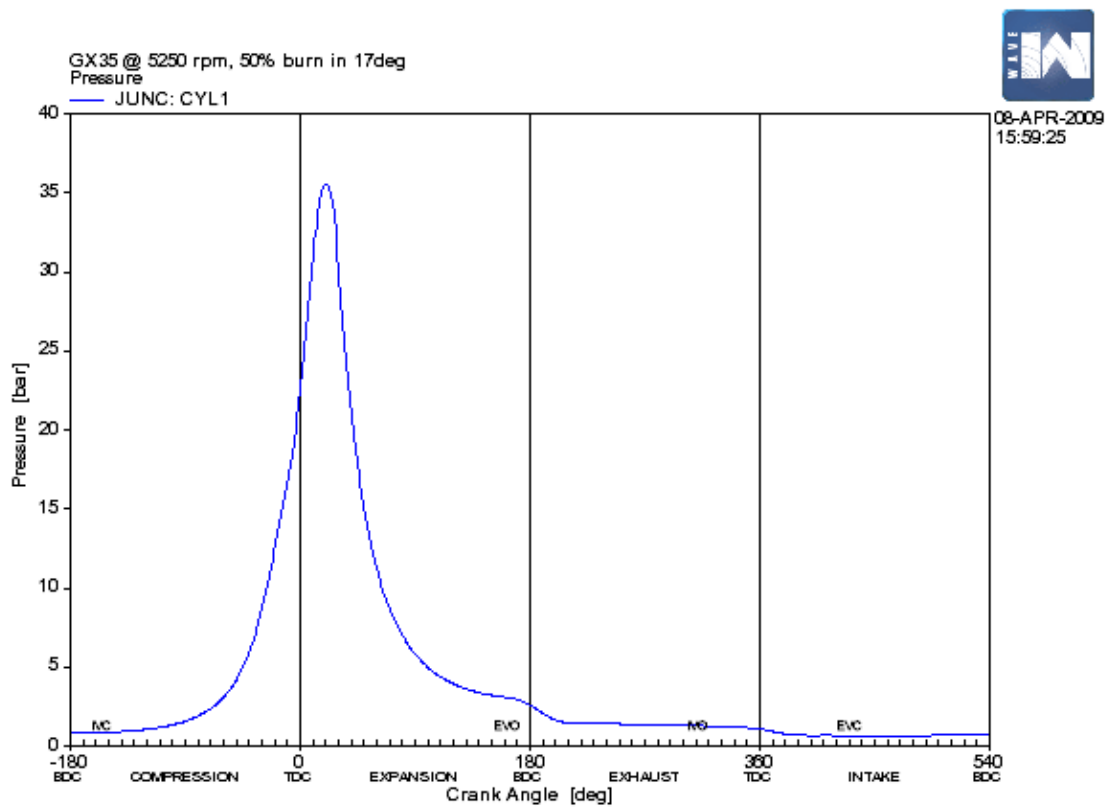


Figure 2. Gas pressure vs. crank angle.

2. LOADS

The load is obtained analytically through the pressure curve presented in Fig. 2. The effects of second order inertia and vertical oscillation of the conrod are not considered in the analysis. Table 2 presents the list of symbols used in the analysis.

Table 2. List of symbols.

Crank angle (°)	φ
Conrod angle (°)	ψ
Conrod length (m)	l
Engine stroke (m)	S
Crank radius (m)	r
Conrod ratio	λ
Rotational speed (rad/s)	ω
Piston inertial force (N)	F_{PISTON}
Gas force (N)	F_{GAS}
Gas pressure (Pa)	p
Conrod axial force (N)	F_{ST}
Radial force on the crankpin (N)	F_R
Lateral force on the crankpin (N)	F_L
Piston vertical translation (m)	x_p

The cranktrain geometry can be seen in Fig 3, where the crank angle r is defined as half of the engine stroke S .

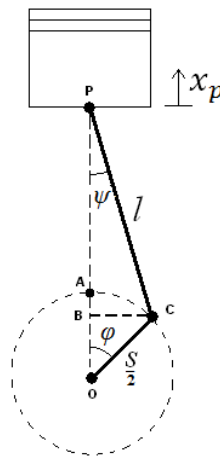


Figure 3. Cranktrain geometry.

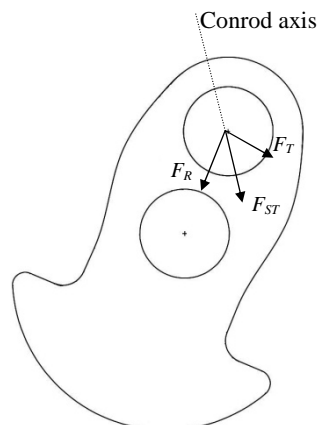


Figure 4. Forces acting on the crankpin.

The piston acceleration, which defines the inertial force of the piston, is evaluated through the Eq. (1), where the conrod ratio is defined as the ratio between the crank radius and the conrod length. The forces acting on the crankshaft pin are evaluated analytically, through the Eqs. (2) to (6) (Basshuyen, Schäfer, 2004). Figure 4 presents the forces acting in the crankpin.

$$\ddot{x}_p = r\omega^2[\cos(\omega t) + \lambda\cos(2\omega t)] \quad (1)$$

$$F_K = F_{GAS} + F_{PISTON} \quad (2)$$

$$F_{GAS} = p(\varphi) \frac{\pi}{4} d^2 \quad (3)$$

$$F_{PISTON} = -m_{PISTON}r\omega^2(\cos\varphi + \lambda\cos 2\varphi) \quad (4)$$

$$F_R = F_{ST}\cos(\varphi + \psi) = F_K \cdot \frac{\cos(\varphi+\psi)}{\cos\psi} \quad (5)$$

$$F_T = F_{ST}\sin(\varphi + \psi) = F_K \cdot \frac{\sin(\varphi+\psi)}{\cos\psi} \quad (6)$$

Table 3 presents the pressure, conrod angle, crank angle and the radial and lateral forces for the condition where the peak gas pressure occurs for maximum torque rotation. However, as a safety measure against imprecision in the evaluation of the operation with ethanol, the loads are evaluated with the using the highest value of peak pressure of the engine (found at 5000 rpm).

Table 3. Values of pressure, conrod angle and crank angle for maximum torque conditions.

Engine rotation (rpm)	Crank angle (°)	Conrod angle (°)	Pressure (MPa)	Radial Force (N)	Lateral Force (N)
5250	24	7	3.5	3650	420

3. TOPOLOGY OPTIMIZATION

Two different approaches are performed by using topology optimization. In the first, the optimization problem consisted in the compliance minimization while attending a maximum volume constraint. The second consisted in the mass (volume) minimization while attending a maximum stress constraint. In both cases the position of the crankshaft center of gravity and the moment of inertia around the crank axis must be kept unchanged. Therefore, the following optimization cases are proposed:

Case A: Objective: minimize compliance
 Constraints: maximum volume fraction, center of gravity position constraint, inertia constraint
 Design variable: design element densities

Case B: Objective: minimize mass (volume)
 Constraints: maximum von Mises stress, center of gravity position constraint, inertia constraint
 Design variable: design element densities

The numerical value of the maximum stress constraint is defined as the yielding strength of the material with a static safety coefficient of 1.6. The material selected for the crankshaft is the AISI 4340 steel, whose relevant properties are summarized in the Tab. 4, and therefore, the maximum von Mises stress allowed in the minimum volume optimization is 290 MPa.

Table 4. Properties of the AISI 4340 steel.

Yielding Strength (GPa)	470
Young's Modulus (GPa)	205
Poisson's ratio	0.3
Density (kg/m ³)	7850

3.1. Optimization Domain

Since the optimized crankshaft is supposed to be interchangeable with the existing one, the geometry of the main bearings, the shaft and the crankpin are considered as non-design volumes, and the design space is restricted by the clearance between the piston skirt and the counterweight. Therefore, the optimization domain comprises the volume around the crankweb and the counterweight.

3.2. Finite Element Model

The finite elements model is built using Altair Hypermesh™ as the mesh generator. The model is discretized into both 8-nodes hexahedral elements and tetrahedral elements mesh.

Two load cases are considered: one which comprises the crankshaft rotational inertia and the compression caused by the combined action of the gas force and the piston inertial force, and another which comprises the crankshaft rotational inertia and the traction caused by the piston inertia. The loads from the gas force and the inertia of the piston are modeled as constant nodal forces applied in the crankpin along a 120° region centered in the conrod axis. The main bearings are constrained in all six degrees of freedom along a 120° region, whose orientation depends on the load case. Figure 5 presents the FE model, for the compression load case.

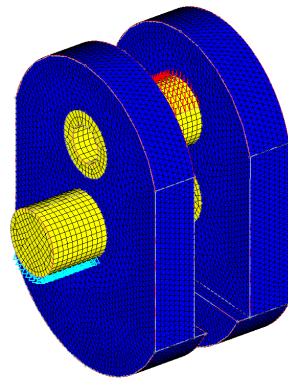


Figure 5. Finite Element Model of the compression load case.

4. RESULTS

The optimization result for case A is presented on Fig. 6.

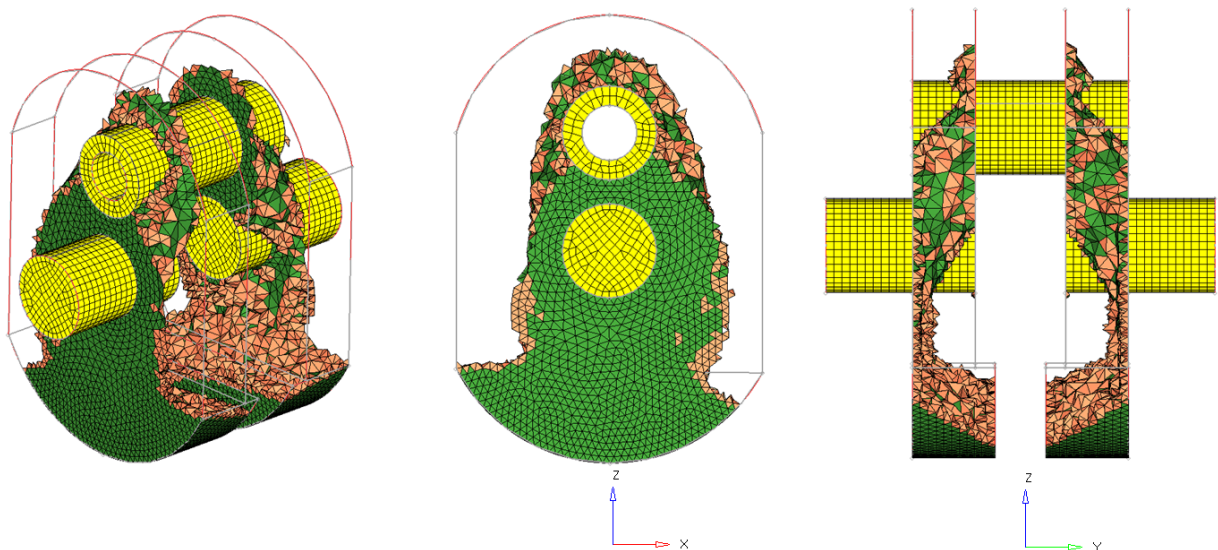


Figure 6. Optimization result for minimum compliance (case A).

Figure 7 presents the result of an optimization for minimal compliance with symmetry constraint around the ZY plane, named case A2.

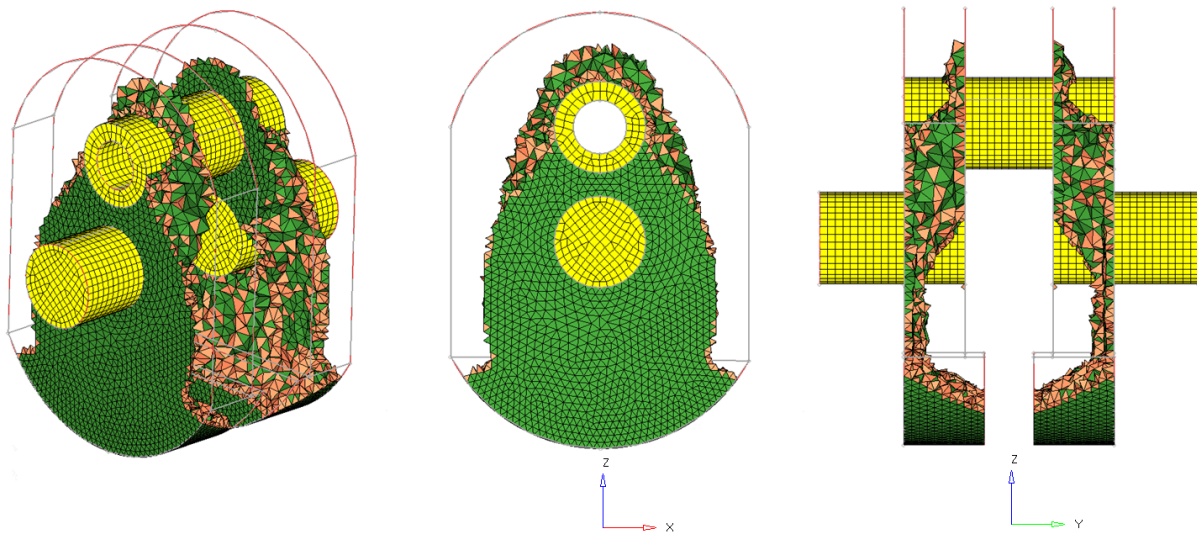


Figure 7. Optimization result for minimum compliance with symmetry constraint (case A2).

The optimization result for minimum volume (case B) is presented in Fig. 8.

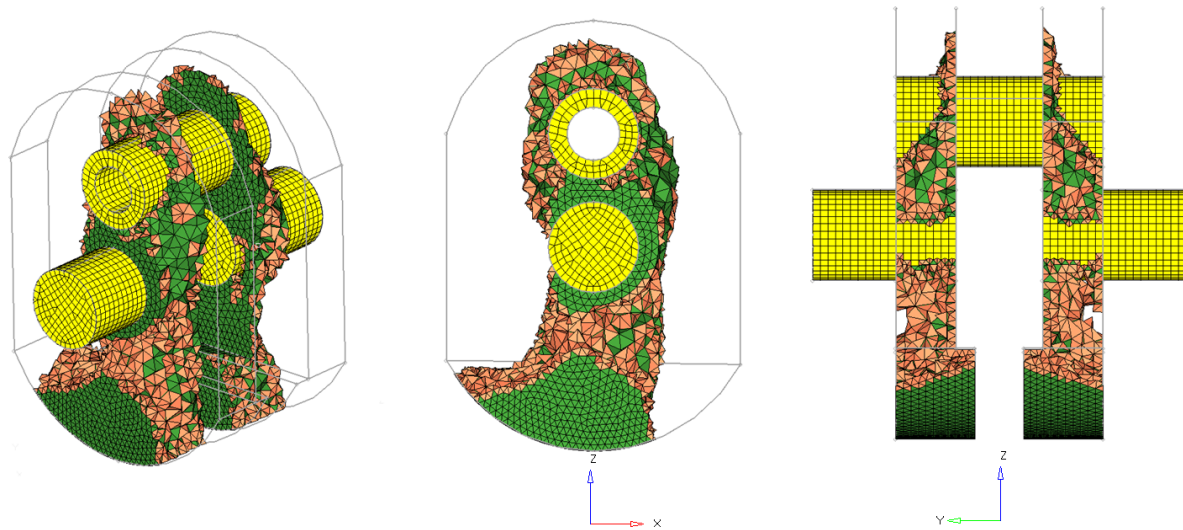


Figure 8. Optimization result for minimum volume (case B).

Figure 9 presents the optimized design for minimal volume with maximum stress and split mold draw direction manufacturing constraint, with the die split in the longitudinal vertical plane (ZY plane) and draw in the horizontal direction (X axis), named case B2.

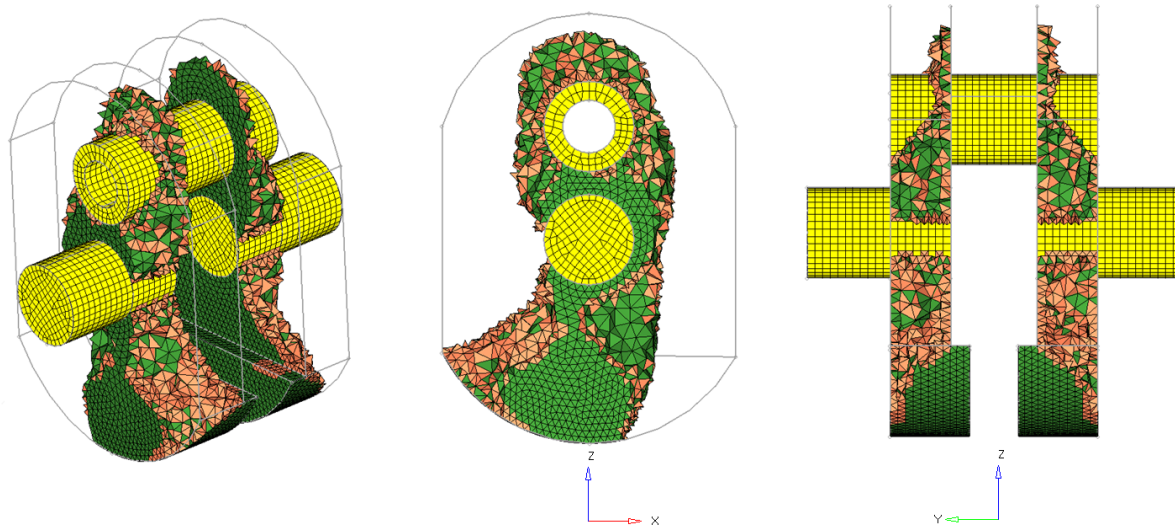


Figure 9. Optimization result for minimum volume and transversal draw direction (case B2).

5. CONCLUSIONS

Two recurrent effects can be observed in the results of cases A and B: the tendency to create an asymmetric structure, due to the absence of the gas force in the traction, and the formation of a chamfer in the crankweb, which exposes the crankpin. The first occurs due to the lack of constraints for the coordinate of the center of gravity in the horizontal plane (red and green directions), and might introduce undesirable unbalancing in the crankshaft. The second, although undesirable for the three-component solution of the original crankshaft, can be directly applied to other concepts, such as a single forged component. This second effect might be diminished for a three-component assembly solution (longitudinal forging) by modeling the interference fit of the crankpin, which would input a local pretension.

The first issue can be solved through the addition of symmetry constraint or additional control of the center of gravity. The case A2 adds a symmetry constraint and although it increases the component mass, its compliance equals the unconstrained design (less than 0.5% difference). Besides, applying the symmetry constraint not only solves the engine balancing issue, but despite the absence of manufacturing constraints the resulting design also presents demolding properties, with a die split in the longitudinal vertical plane (ZY plane) and draw in the horizontal direction (X axis).

The resulting design for the minimum volume (case B) allows further reduction of the component mass (115.5g) but also inputs additional unbalance. Also, the topology of the counterweight does not allow forging in any direction, so it is necessary the addition of manufacturing constraints for a feasible design. This feasibility is accomplished by inserting a draw direction constraint in the transversal direction, with mold split in the vertical plane (ZY plane) and horizontal draw direction (X axis). The addition of this manufacturing constraint resulted in an increased component mass.

Table 5 presents a comparison of the resulting designs for each case. When considered the feasibility of the design and the engine balancing, the case A2 shows the more promising result.

Table 5. Comparison between the results of the optimization cases.

Case	Objective	Constraint	Manufacturing Constraint	Mass	Mass reduction ⁽¹⁾
A	Min compliance	Vol frac < 0.4	-	118.5g	32.7%
A2	Min compliance	Vol frac < 0.4	Symmetry	123.6g	29.8%
B	Min Volume	Stress < 290MPa	-	115.5g	34.4%
B2	Min Volume	Stress < 290MPa	Draw	126.4g	28.2%

(1): referenced to the mass of the original crankshaft of 176g

6. ACKNOWLEDGEMENTS

The first and second authors thanks ThyssenKrupp Metalúrgica Campo Limpo (Campo Limpo – São Paulo – Brazil) for supporting him through a scholarship. Third author thanks ThyssenKrupp Metalúrgica Campo Limpo for the cooperation program. All authors thanks FDTE – Fundação para o Desenvolvimento Tecnológico da Engenharia (FDTE – Foundation for the Technological Development of Engineering – São Paulo – Brazil) for the administration of the

cooperation program, Altair Engineering do Brasil for the licenses and technical support on Altair Engineering Softwares and Robtec for the digitalization of the engine components.

7. REFERENCES

- Basshuyen, R., Schäfer, F., 2004, "Internal Combustion Engine Handbook: Basics, Components, Systems and Perspectives", SAE International, Warrendale, 868 p.
- Bendsøe, M. P., Sigmund, O., 2003, "Topology Optimization: Theory, Methods and Applications", Springer, 370p.
- Ganpule, S., Mate, S., Gokhale, U. R., 2006, "Finite Element Analysis Approach for Crankshaft Optimization", Altair "India/ASEAN" CAE users conference 2006, Bangalore.
- Heywood, J. B., 1988, "Internal Combustion Engine Fundamentals", McGraw-Hill, 930p.
- Mendes, A. S., Meirelles, P. S., Zampiere, D. E., 2005, "Desenvolvimento e Validação de Metodologia para Análise de Vibrações Torsionais em Motores de Combustão Interna", Master's Thesis – Universidade Estadual de Campinas, Campinas, 132p.
- Montazersadgh, F. H., Fatemi, A., 2009, "Optimization of a Forged Steel Crankshaft Subject to Dynamic Loading", SAE International Journal of Materials & Manufacturing, Vol 1, pp. 211-217.

8. RESPONSIBILITY NOTICE

The authors are the only responsible for the printed material included in this paper.